EUROPEAN SYNCHROTRON RADIATION FACILITY

INSTALLATION EUROPEENNE DE RAYONNEMENT SYNCHROTRON

ESRF

Experiment Report Form

The double page inside this form is to be filled in by all users or groups of users who have had access to beam time for measurements at the ESRF.

Once completed, the report should be submitted electronically to the User Office via the User Portal:

https://wwws.esrf.fr/misapps/SMISWebClient/protected/welcome.do

Reports supporting requests for additional beam time

Reports can be submitted independently of new proposals – it is necessary simply to indicate the number of the report(s) supporting a new proposal on the proposal form.

The Review Committees reserve the right to reject new proposals from groups who have not reported on the use of beam time allocated previously.

Reports on experiments relating to long term projects

Proposers awarded beam time for a long term project are required to submit an interim report at the end of each year, irrespective of the number of shifts of beam time they have used.

Published papers

All users must give proper credit to ESRF staff members and proper mention to ESRF facilities which were essential for the results described in any ensuing publication. Further, they are obliged to send to the Joint ESRF/ ILL library the complete reference and the abstract of all papers appearing in print, and resulting from the use of the ESRF.

Should you wish to make more general comments on the experiment, please note them on the User Evaluation Form, and send both the Report and the Evaluation Form to the User Office.

Deadlines for submission of Experimental Reports

- 1st March for experiments carried out up until June of the previous year;
- 1st September for experiments carried out up until January of the same year.

Instructions for preparing your Report

- fill in a separate form for each project or series of measurements.
- type your report, in English.
- include the reference number of the proposal to which the report refers.
- make sure that the text, tables and figures fit into the space available.
- if your work is published or is in press, you may prefer to paste in the abstract, and add full reference details. If the abstract is in a language other than English, please include an English translation.

ESRF	**Experiment title:** Effects of Mn-reducing treatments on the integrity of glass corrosion bodies	**Experiment number**: EC873
Beamline: ID21	**Date of experiment**: from: 02/11/2011 to: 05/11/2011	**Date of report**: 14/09/2011
Shifts: 9	**Local contact(s)**: Dr. Giulia Veronesi	*Received at ESRF:*

Names and affiliations of applicants (* indicates experimentalists):

Simone Cagno – University of Antwerp*
Gert Nuyts – University of Antwerp*
Kevin Hellemans – University of Antwerp*
Koen Janssens – Universiteit Antwerpen

Report:

Introduction

The speed and nature of the glass corrosion process depend both on the characteristics of the glass and on environmental conditions; an influence can also be exerted by micro-organisms, vibrations, and possible earlier conservation treatments. The weathering of silicate glasses is caused by a series of physico-chemical transformations occurring in presence of water (1). The first step is the penetration, via molecular diffusion and/or reversible hydrolysis/condensation reactions, of molecular water into the glass. During this process, the silicate network is reported to experience structural transformations (2).

$\equiv Si-O-Si\equiv \; + \; H_2O_{(aq)} \rightarrow 2 \equiv Si-OH$

$2 \equiv Si-OH \rightarrow \; \equiv Si-O-Si\equiv \; + \; H_2O_{(glass)}$

The second step of glass weathering is the ion exchange, that is the leaching of the most mobile cations from the glass and their substitution by protons (3). The mobility of the cations depends on charge, size and glass composition. As a result, some glass compositions (e.g. silica-rich glasses) are more resistant to leaching than others. The ions removed from the glass structure can also form weathering products (e.g. sulphates, chlorides, etc.) on the glass surface when their solubility products are exceeded in the water film on the surface (4-5).

$\equiv Si-O^-M^+_{(glass)} \; + H^+_{(aq)} \rightarrow \; \equiv Si-O^-H^+_{(glass)} \; + M^+_{(aq)}$

When the water in close contact with the glass is not regularly replenished (alternate wet/dry conditions), the pH of the aqueous solution will increase, due to the ongoing ion-exchange. When pH values exceed the value of 9, the third step of glass weathering occurs: the silicate network is attacked by the hydroxyl ions.

$\equiv Si-O-Si \equiv + \, OH^-_{(aq)} \rightarrow \equiv Si-OH + \equiv Si-O^-$

$\equiv Si-O^- + H_2O_{(aq)} \rightarrow \; \equiv Si-OH + OH^-_{(aq)}$

These three steps cause a leached layer to be formed, with a cation-depleted network that is structurally weakened, and that has a lower density than the original glass. If no change in environmental conditions intervenes, the so-called leached layer will gradually increase in thickness and the stress across the interface between altered and healthy glass will cause thin layers of altered glass to crack off. This physical process in turn exposes a new surface of fresh glass to the weathering agents. By a succession of such events, stacks of µm-thin lamellae of leached-out glass, interspersed with voids, can be formed. Due to interference phenomena, the multilayered material can obtain an iridescent aspect when t the inter-lamellar voids are not water-filled.

With the aim of characterizing the speed of alteration of different glass compositions under diverse weathering environments, in the present experiment SR-µFTIR reflectance spectroscopy has been selected as technique of choice. Different techniques can be used to determine the corrosion rate of glass and the alteration products (e.g. XRF, SEM-EDS), but SR-μFTIR reflectance spectroscopy appears promising for a number of factors. First, recent papers on FTIR applications on glass show that it is relatively easy to differentiate healthy from altered glass (1-9) in reason of the significant changes in the FTIR spectra (shift and disappearance of the Si-O$^-$ stretching peak between 900 and 1000 cm^{-1}, shift and increase of the Si-O-Si stretching peak(s) in the region 1050-1250 cm^{-1}, appearance of a Si-OH vibration peak around 900 cm^{-1}) induced by alteration (6-7-8). Secondly, the high sensitivity and specificity can allow detecting even small amount of secondary alteration products in the initial precipitation areas (e.g. $CaCO_3$, MnO_2). Finally, the high flux and high lateral resolution will allow obtaining high resolution maps in a reasonable amount of time, that is crucial, seen the iterative nature of the experiment described below.

Preparation

The sample preparation is schematically represented in Figure 1. From a large piece of sensor glass (Fraunhöfer M1.0) smaller parts were cut using a pair of glass pliers. These smaller sample were then put in an acidic solution (pH 0,2,4 or 7) for a variable amount of time. After the sample were treated with the acidic solution, they were then put in a 0.05 M $MnCl_2$ – solution for 24h or 48h. Although the presence of manganese can not be proven from SR-FTIR techniques, we simultaneously acquired beamtime at the SXM endstation as well, thus allowing us to both proof the formation of a leached layer and the presence and oxidation state of manganese.

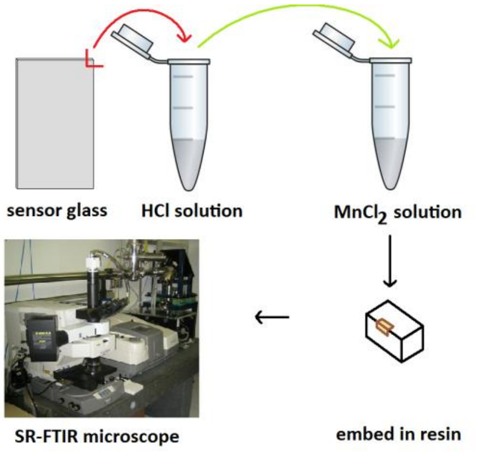

Figure 1: Sample preparation

Results

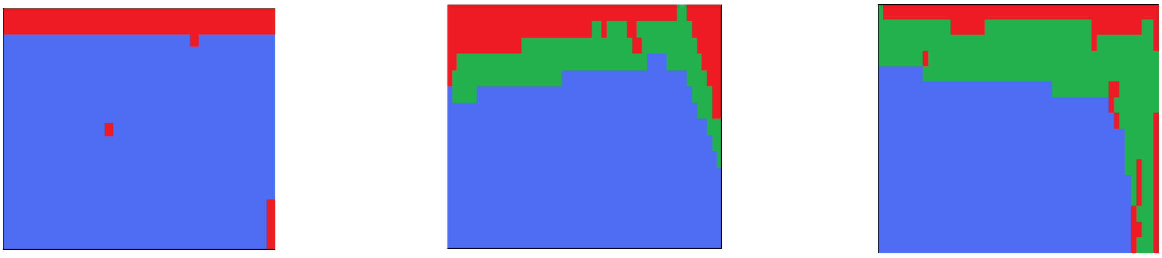

(a) (b) (c)

Figure 2: Cluster analysis map after (a) 0h, (b) 3h and (c) 6h in 1M HCl solution (blue = original glass, green = corroded glass, red = resin)

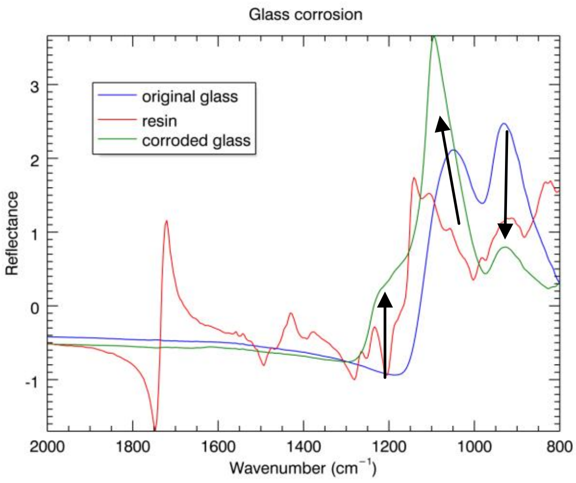

Figure 3: average spectra of clusters

The glass samples were measured in reflection mode (800 cm^{-1} – 4000 cm^{-1}, 50 spectra per point) using the Thermo Scientific scanning FTIR microscope. On the resulting maps, cluster analysis was performed with Cytospec. From the cluster maps (Figure 2) it becomes evident that the leached layer grows rapidly in strong acidic conditions. The average spectra for each cluster is given below in Figure 3, confirming our previous assumptions about the designation of the clusters. The resin shows a carbonylic band around 1700 cm^{-1}, the original glass shows a strong Si-O$^-$ stretching band between 900 and 1000 cm^{-1}, whereas the leached layer can be identified by the increasing Si-O-Si bands around 1100 and 1250 cm^{-1}.

In order to assess the validity of our results it is of great importance to investigate whether or not similar behaviour occurs under less acidic conditions, as real-life samples usually do not undergo such harsh conditions. Therefore the experiment was also performed using a HCl solution with higher pH values. Results show that corrosion already sets in after 4h in a pH 4 solution (Figure 4a), comparable to acid rain. As can be expected, no significant deterioration was observed at neutral pH within the timeframe of the experiment (Figure 4b).

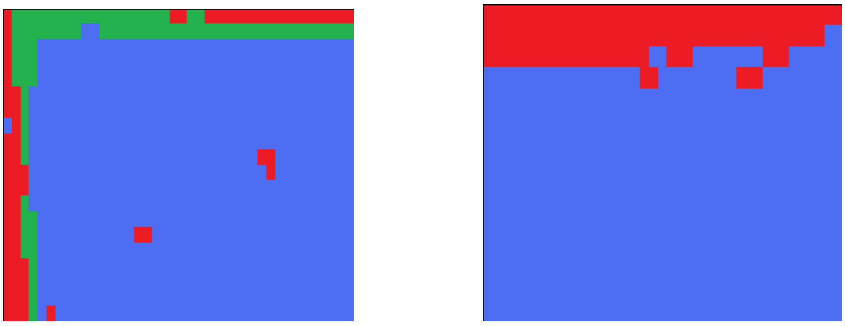

(a) (b)

Figure 4: Corrosion in sensorglass after (a) 4h in a pH 4 solution and (b) 6h in a pH 7 solution (blue = original glass, green = corroded glass, red = resin)

SR-FTIR also allowed us to determine that no significant changes to the leached layer can be observed, except for the small change described by Ethridge et al. (9) to the band at 1200 cm^{-1}, which becomes slightly more intense, as can be seen in Fig. 5. Furthermore, it was shown that the leached layer reaches a maximal depth of 40-50 µm, possibly due to the limited diffusion through the increasing thickness of the leached layer.

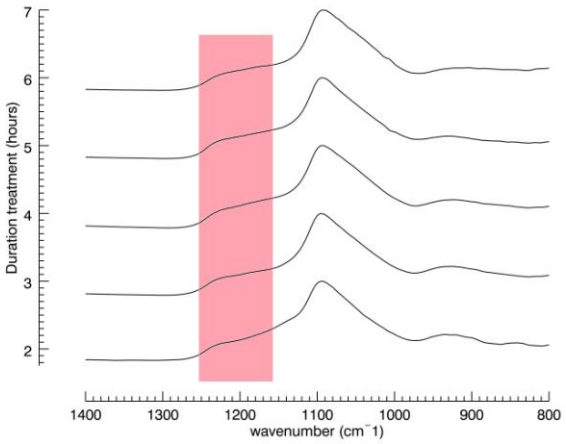

Figure 5: spectrum of leached layer as a function of treatment time

Conclusion and future

The use of SR-FTIR allowed us to study the formation of a leached layer on glass under acidic conditions, which would not have been possible in traditional macro-FTIR techniques. Moreover, the high flux of the IR beam proved vital to obtain spectra in a fast and reliable manner, as the experiment might have taken weeks to complete with common IR sources. We can conclude that leaching of glass can occur in even slightly acidic environments, giving rise to the need of treatments for this effect.

References

(1) J. Am. Ceram. Soc. (2008) 91:728–35; (2) Earth Planet. Sci. Lett. (1998) 163:43–51; (3) Anal. Bioanal. Chem. (2004) 379:628-39; (4) J. Non-Cryst. Solids (2006) 352:368-79; (5) Microchim. Acta (2000) 135:121-30; (6) Silicon (2010) 2:41-7; (7) J. Non-Cryst. Solids (2007) 353:2667-74; (8) J. Non Cryst. Solids (2009) 355:1630-7; (9) E.C. Ethridge, Mechanics and kinetics of Binary Alkali Silicate Glass Corrosion, (diss,1977).